Site and Morphology Controlled ZnO Deposition on Pd Catalyst Prepared from Pd/PMMA Thin Film Using UV Lithography

Jae-Young Lee, Dehui Yin, and Shin Horiuchi*

Nanotechnology Research Institute, National Institute of Advanced Industrial Science and Technology (AIST), 1-1-1, Higashi, Tsukuba, Ibaraki 305-8565, Japan

Received March 25, 2005. Revised Manuscript Received August 4, 2005

Well-defined line patterns of zinc oxide (ZnO) were site-selectively grown on the photopatterned palladium (Pd) catalysts through an electroless deposition process under mild conditions. Pd catalysts in the form of nanoparticles were mainly positioned on the UV irradiated surface of polymethyl methacrylate (PMMA) film via the reduction of vaporized palladium(II) bis(acetylacetonato) denoted as $Pd(acac)_2$ in our drying process. The catalytic activity of the Pd nanoparticles was affected by the PMMA film thickness, the UV dose, and the exposure time to $Pd(acac)_2$, whose optimum values were ca. 20 nm, 20 J/cm^2, and 5 min, respectively. The ZnO pattern accuracy and the crystalline morphology were varied sensitively depending on the Pd particle size and deposition temperature, in which the former caused the fatter crystals, while the latter suppressed the lateral growth, giving the longer hexagonal nanorods.

Introduction

Zinc oxide (ZnO) film has been extensively investigated for many applications such as phosphors in a high-resolution field emission display, transparent conducting electrodes, solar cell windows, and surface acoustic wave devices.[1−5] ZnO films are prepared by several methods using various physical, chemical, photochemical, and electrochemical methods, which are mainly divided into two classes: solid−vapor phase growth and solution phase synthesis.[6,7] Among the former, vapor−liquid−solid (VLS), chemical vapor deposition (CVD), and thermal evaporation methods are mainly used to produce various high-quality ZnO structures, but their major limitations are complex process, rigid experimental conditions, and low yield. Therefore, the latter has become a promising option for large-scale production due to its simple, fast, and less expensive virtues.

Electroless deposition technique is a sort of solution phase method having many merits as follows:[2,3,8,9] (1) it is a simple and economical low-energy process, (2) it allows us to obtain uniformly thick coatings of metallic, dielectric, and semiconducting materials deposited on both conducting and nonconducting substrates, (3) it can be applied to the complex three-dimensional surfaces, even if they are hardly accessible surfaces, and (4) the deposited thin films and the substrates are safe from the thermal stress because it is performed under 100 °C.

To carry out electroless deposition, the substrate's surface should be given the sensitization and subsequent activation by the catalysts prior to the deposition process. Conventionally, palladium (Pd) catalyst has been employed to activate the surface of the substrate by dipping it into $SnCl_2$ and $PdCl_2$ aqueous solutions, respectively.[10] To create the pattern using the conventional film deposited, a two-step process is typically employed: first, the deposited film is coated by a photoresist and a pattern is defined on the photoresist by UV lithography, and second, the pattern is transferred onto the deposited film by a reactive ion etching process. Recently, researchers have investigated carrying it out under mild conditions as compared to the conventional etching methods and advancing the micro- and nanopatterning of catalysts, on which the direct deposition can be done site-selectively, by combining photochemical, catalytic, and self-assembled block copolymer tools.[2,8,11−13] For example, photopatternable self-assembled monolayers (SAM) have been employed to get patterned metallic catalysts.[2,8,12] UV light passing a photomask changes the UV-sensitive groups of the SAM, so the metallic catalysts can be selectively attached to the catalyst-attractive surface with reproducing the photomask pattern. Saito et al.[2,8] fabricated an electroless ZnO micropatterning on the Pd catalyst by employing a photopatterned phenyltrichlorosilane SAM. UV light through a photomask

* Corresponding author. E-mail: s.horiuchi@aist.go.jp. Tel: +81-3-3588-8309. Fax: +81-3-3599-8166.

(1) Tian, Z. T.; Voigt, J. A.; Liu, J.; Mckenzie, B.; Mcdermott, M. J.; Rodriguez, M. A.; Konishi, H.; Xu, H. *Nat. Mater.* **2003**, *2*, 821−826.
(2) Saito, N.; Haneda, H.; Sekiguchi, T.; Ohashi, N.; Sakaguchi, I.; Koumoto, K. *Adv. Mater.* **2002**, *14*, 418−421.
(3) Izaki, M.; Katayama, J. *J. Electrochem. Soc.* **2000**, *147*, 210−213.
(4) Gordillo, G. *Surf. Rev. Lett.* **2002**, *9*, 1675−1680.
(5) Muthukumar, S.; Gorla, C. R.; Emanetoglu, N. W.; Liang, S.; Lu, Y. *J. Cryst. Growth* **2001**, *225*, 197−210.
(6) Wang, Z.; Qian, X. F.; Yin, J.; Zhu, Z. K. *Langmuir* **2004**, *20*, 3441−3448.
(7) Li, F.; Ding, Y.; Gao, P.; Xin, X.; Wang, Z. L. *Angew. Chem.* **2004**, *116*, 5350−5354.
(8) Saito, N.; Haneda, H.; Seo, W. S.; Koumoto, K. *Langmuir* **2001**, *17*, 1461−1469.
(9) Elshabini, A. A. R.; Barlow, F. D. *Thin Film Technology Handbook*; McGraw-Hill: New York, 1997; Chapter 1.
(10) Khoperia, T. N.; Tabatadze, T. J.; Zedgenize, T. I. *Electrochim. Acta* **1997**, *42*, 3049−3055.
(11) Yamabi, S.; Imai, H. *J. Mater. Chem.* **2002**, *12*, 3773−3778.
(12) Sugimura, H.; Hanji, T.; Takao, O.; Masuda, T.; Misawa, H. *Electrochim. Acta* **2001**, *47*, 103−107.
(13) Masuda, Y.; Seo, W. S.; Koumoto, K. *Langmuir* **2001**, *17*, 4876−4880.

10.1021/cm0506555 CCC: $30.25 © 2005 American Chemical Society
Published on Web 09/29/2005

changed the phenyl groups of the SAM to OH groups, and then the Pd catalysts were selectively attached on the surface of phenyl groups in $SnCl_2$ and $PdCl_2$ aqueous solutions. Sugimura et al.[12] reported the success of Ni pattern on the UV patterned Pd catalysts using an octadecyltrimethoxysilane SAM in which the catalysts were produced in $PdCl_2$/HCl/HF solution.

We have developed a simple dry process for the patterning of metal catalysts such as Pd, Pt, and Co into the polymer films through the reduction of metal complexes used as precursors.[14−16] For example, palladium(II) bis(acetylacetonato) complex denoted as $Pd(acac)_2$ was vaporized at 180 °C in nitrogen atmosphere and the vapor penetrated into the polymers. Then, they adsorbed on the nucleophilic groups in polymer chains and reduced to the Pd metals in the form of nanoclusters. When a block copolymer was used as a polymer film, Pd nanoparticles were selectively generated in the Pd-attractive microdomains. We also found that the reduction rate of the $Pd(acac)_2$ in poly(methyl methacrylate) (PMMA) film was too low to generate sufficient Pd nanoparticles; however, if PMMA film was treated with UV irradiation prior to the exposure to $Pd(acac)_2$ vapor, the reduction rate was largely modified.[15] Therefore, UV irradiation through a photomask could produce the Pd pattern on PMMA film. However, almost all Pd nanoparticles are generated under the polymer surface. Therefore, the nanoparticles should be disclosed to the surface to give them catalytic activity.

In this paper, we adjusted the PMMA film thickness, the UV dose, and the exposure time to $Pd(acac)_2$ so that the upper sides of the patterned Pd catalysts could be revealed onto the surface of the film in order to use them as catalysts for the deposition of ZnO, and we reported the effects of the particle size of Pd catalyst and the deposition temperature on the ZnO pattern accuracy and the crystalline morphology in the electroless deposition process using the aqueous solution of $Zn(NO_3)_2$ with dimethylamine borane (DMAB).[2,8]

Experimental Section

Materials. $Pd(acac)_2$ was purchased from Johnson Matthey Materials Technology and was recrystallized in acetone. Poly(methyl methacrylate) (PMMA) was obtained from Aldrich Chemical Co., Inc., whose number-average molecular weight, Mn, was 350000. It was precipitated twice from methylene chloride into methyl alcohol for purification. Zinc nitrate ($Zn(NO_3)_2$) and dimethylamine borane (DMAB) were purchased from Wako Pure Chemical Industries, Ltd.

Synthesis of ZnO Patterning. The procedure for ZnO deposition on the UV-patterned Pd catalysts was shown in Figure 1. First, ca. 20 nm thick PMMA thin film was prepared on the O_2 plasma-cleaned Si wafer with 0.75 wt % PMMA/toluene solution using a spin coater and dried at 60 °C for 2 h in a vacuum oven. And then, UV light ranging from 240 to 300 nm was irradiated on the PMMA surface with the dose of 20 J/cm^2 through a photomask, in which lines of 2 μm width were open with 5 μm spaces. The UV irradiation was employed using a spot light source, Lightningcure LC6 (Hamamatsu Photonics K. K.), attached with a flexible light-guide emitting UV light from a mercury−xenon lamp, and the PMMA film was stimulated at a distance of 5 cm from light-guide end, giving the UV intensity of 100 mW/cm^2 at 250 nm.

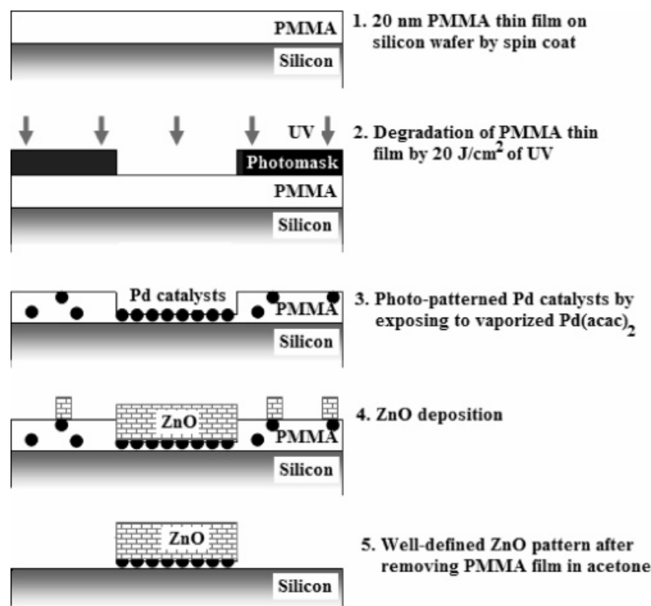

Figure 1. Schematic illustration for ZnO deposition on the UV-patterned Pd catalysts.

To pattern Pd catalysts on the UV irradiated area, the following procedure was used, as described in our previous paper:[14−16] Ten milligrams of $Pd(acac)_2$ in the glass tube reactor was sublimed at 180 °C in vacuo and condensed on the upper side of the glass wall. Then the UV patterned PMMA/Si wafer was placed into the reactor and maintained at 180 °C of N_2 atmosphere for 3, 5, 10, and 30 min, respectively. In this stage, Pd catalysts were mostly positioned on the UV irradiated area.

To make the ZnO crystals grow site-selectively on the Pd catalysts, Pd-patterned PMMA/Si wafer was soaked in an aqueous solution of 0.05 M $Zn(NO_3)_2$ and 0.05 M DMAB at 50, 60, 70, and 80 °C for various times, and the misdeposited ZnO on the UV masked area was completely removed from the Si surface during stripping off of the PMMA film in acetone for 3 min at room temperature.

Instrumental Analysis. X-ray photoelectron spectroscopy (XPS) spectra were acquired on a PHI's Quantum 2000 Scanning ESCA Microbe (ULVAC-PHI Inc., Japan) equipped with a hemispherical capacitor analyzer using monochromated Al Kα radiation at an angle of 45° between the analyzer axis and the sample normal. All analyses were performed at a constant pass energy of 117.4 eV for general survey and the measured binding energies were corrected referring to the binding energy of C 1s in CH_2 (284.6 eV). Energy-filtering transmission electron microscopy (EFTEM, LEO922 operated at an accelerating voltage of 200 kV) was employed to get zero-loss images, which is equivalent to conventional TEM images, selected area electron diffraction (SAED), and elemental mapping data, and the line patterns and morphologies of ZnO were observed by scanning electron microscopy (SEM, Philips XL30 FE-SEM) at an acceleration voltage of 10 kV. The distribution density of Pd nanoparticles, ZnO deposition area percentage, and the number-average diameters were statistically estimated by the image processing software (analySIS, Soft Imaging System Co. Ltd.). A multilayer analyses method in a JASCO M-220 spectroscopic ellipsometer was performed to measure the PMMA film

(14) Yin, D.; Horiuchi, S.; Masuoka, T. *Chem. Mater.* **2005**, *17*, 463−469.
(15) Horiuchi, S.; Fujita, T.; Hayakawa, T.; Nakao, Y. *Adv. Mater.* **2003**, *15*, 1449−1452.
(16) Horiuchi, S.; Fujita, T.; Hayakawa, T.; Nakao, Y. *Langmuir* **2003**, *19*, 2963−2973.

thickness using the relation between the polarization change and the refractive index and film thickness. The height of the deposited ZnO was measured by a scanning force microscopy (SFM, SPA 300HV, Seiko Instruments, Inc.) in a tapping mode using a cantilever (SI-AF01, Seiko Instruments Inc., spring constant of 0.15 N/m).

Results and Discussion

The ZnO growth was affected by various factors such as the distribution of Pd catalysts, deposition temperature and time, reagents formulation, and the species of substrate, and our research here was focused on the first one. The particle size of Pd catalyst and its distribution density varied according to the PMMA film thickness, the UV dose, and the exposure time to $Pd(acac)_2$ vapor, and we found in the preliminary experiment that the optimum PMMA thickness and the UV dose were ca. 20 nm and 20 J/cm^2, respectively. If the PMMA film was thicker than 20 nm, most Pd catalysts were formed under the film surface, so the catalytic activity was covered by the film. However, if it was thinner than 20 nm, UV dose removed almost all the PMMA film through the breakage and gasification of the chains together with C═C double bond, so it was also against the formation of Pd nanoparticles. When UV dose was 20 J/cm^2, SFM measurement showed that ca. 15 nm was removed from ca. 20 nm thick PMMA surface.

To observe the Pd nanoparticles, ca. 20 nm thick PMMA film was spin-coated on a cleaved NaCl crystal followed by UV irradiation, and then it was exposed to $Pd(acac)_2$ vapor for various times. After the exposure, the Pd incorporated PMMA films were lifted off from the NaCl by dipping it into water and were mounted on 600 mesh TEM copper grids, which were preliminary coated with carbon film by dipping the carbon-coated NaCl into water.

TEM images in Figure 2a−d show the Pd nanoparticles in the UV irradiated area whose exposure times to $Pd(acac)_2$ vapor were 3, 5, 10, and 30 min, respectively, where black spots were the Pd nanoparticles in the form of nanocluster. All surfaces are evenly covered by the black spots with high distribution density. This implies that C═C double bonds generated by UV irradiation played an important role in the reduction of $Pd(acac)_2$.[15,17,18] To estimate the distribution properties, the TEM images were introduced to image analyzer. As the exposure time increased, the number-average diameter increased, showing the shift of the distribution curve to the right-hand side; however, the number of particles per 1000 nm^2 decreased except in the case of 5 min. On the other hand, the area % of the Pd nanoparticles increased in a short time of 5 min and became almost constant after that time. These results say that the nucleation is initiated under a very short time of 3 min and they grow quickly until 5 min. After that time, they aggregate one another without the new nucleation, giving larger particle size and lower number of particles because the small Pd particles were maybe gathered by the macro Brownian motion of PMMA chains

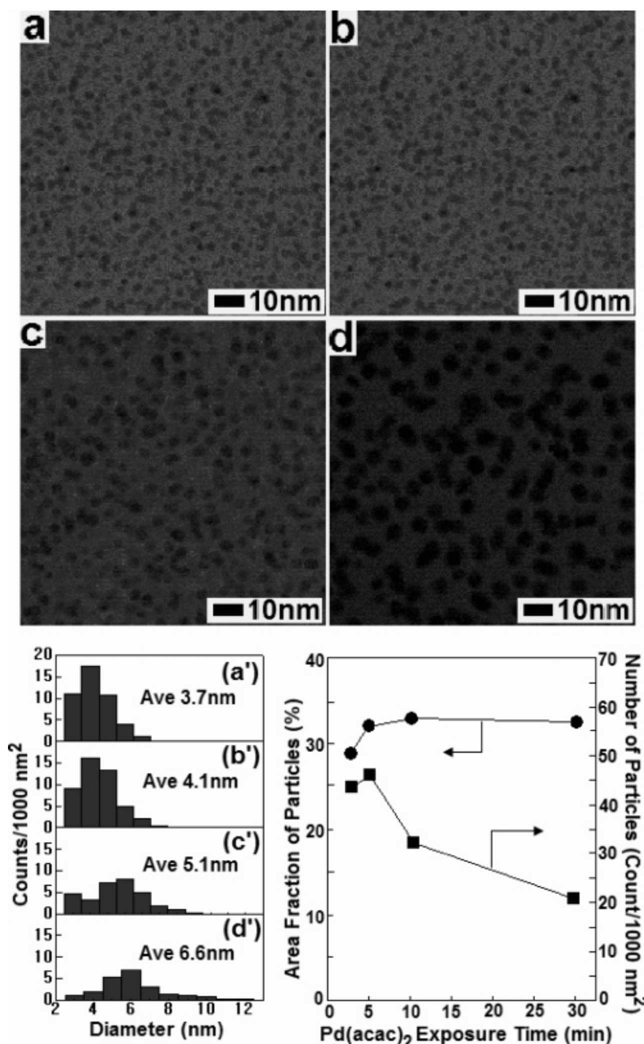

Figure 2. Effect of exposure time to $Pd(acac)_2$ vapor on the distribution of Pd nanoparticles on the surface of PMMA thin film. (a−d) TEM images on the UV irradiated area were prepared by exposure to $Pd(acac)_2$ vapor for 3, 5, 10, and 30 min, respectively; (a′−d′) particle size distribution of each TEM image; effects of the exposure time on the area % of Pd particles or number of particles/1000 nm^2.

at far higher reduction temperature (180 °C) than the glass transition temperature (105 °C).

Figure 3 shows the SEM images of well-defined ZnO patterns and the magnified boundary areas deposited (a, b) at 50 °C for 20 min or (c, d) at 80 °C for 5 min in an aqueous solution of 0.05 M $Zn(NO_3)_2$ and 0.05 M DMAB, in which they were deposited on the Pd catalysts of 5 min exposure to $Pd(acac)_2$ vapor. The overall line patterns reproduced the photomask pattern regardless of deposition temperature. The contrast between the UV irradiated (bright line) and the masked area was significantly enhanced through the deposition process, suggesting that ZnO crystals were deposited with an excellent site selectivity on the Pd patterns. Figure 3b,d shows that the ZnO boundary was clearly divided into UV irradiated and masked area. The UV irradiated area was covered by the dense continuous particles, while no particles were on the UV masked area. In fact, there was about 15% error in the ZnO pattern right after the deposition process because some Pd catalysts disclosed onto the UV masked surface initiated the ZnO growth. However, this error could be cleaned together with PMMA film in acetone during the

(17) Aymonier, C.; Bortzmeyer, D.; Thomann, R.; Mülhaupt, R. *Chem. Mater.* **2003**, *15*, 4874−4878.
(18) Chan, Y. N. C.; Craig, G. S. W.; Schrock, R. R.; Cohen, R. E. *Chem. Mater.* **1992**, *4*, 885−894.

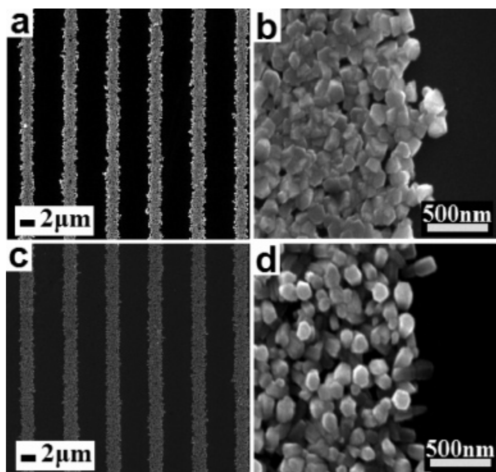

Figure 3. SEM images of ZnO pattern and the magnified boundary area. (a,b) were deposited at 50 °C for 20 min and (c,b) were done at 80 °C for 5 min in an aqueous solution of 0.05 M $Zn(NO_3)_2$ and 0.05 M DMAB, where Pd catalysts were prepared by exposure to $Pd(acac)_2$ vapor for 5 min.

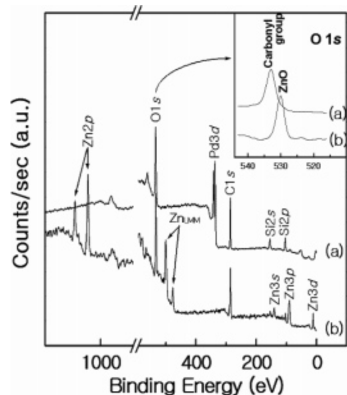

Figure 4. XPS spectra for (a) Pd-incorporated PMMA without pattern and (b) ZnO thin film prepared at 50 °C for 10 min in an aqueous solution of 0.05 M $Zn(NO_3)_2$ and 0.05 M DMAB, where Pd catalysts were prepared on the UV irradiated area by exposure to $Pd(acac)_2$ vapor for 5 min.

last stripping process. Nevertheless, to expand the usefulness of this technique, misdeposition on the UV masked area must be prevented. So we are now searching for a new polymer producing accurate Pd-rich and Pd-free patterns by UV irradiation.

Root-mean-square (rms) edge roughness measured from Figure 3b,d were ca. 150 nm and ca. 95 nm, respectively, and these values can be improved by using a better light source and photomask because our UV light was not a laser and photomask was handmade, so edge lines for Pd catalysts were produced with rough. We also found that edge acuity increased with the decreasing line width. The morphology of the ZnO particles synthesized at 50 °C was mostly consisted of short faceted hexagonal nanorods as shown in Figure 3b, while that of 80 °C was columnar hexagonal nanorods as shown in Figure 3d.

With the help of XPS, EFTEM, and SAED techniques, it was confirmed that ZnO crystals were site-selectively deposited on the Pd catalysts. Figure 4 is the XPS spectra for (a) Pd incorporated PMMA without pattern and (b) ZnO thin film fabricated at 50 °C for 10 min showing the characteristic peaks of the core levels of Zn 2p, O 1s, and Pd 3d. In spectrum (a), the binding energy (BE) of Pd 3d

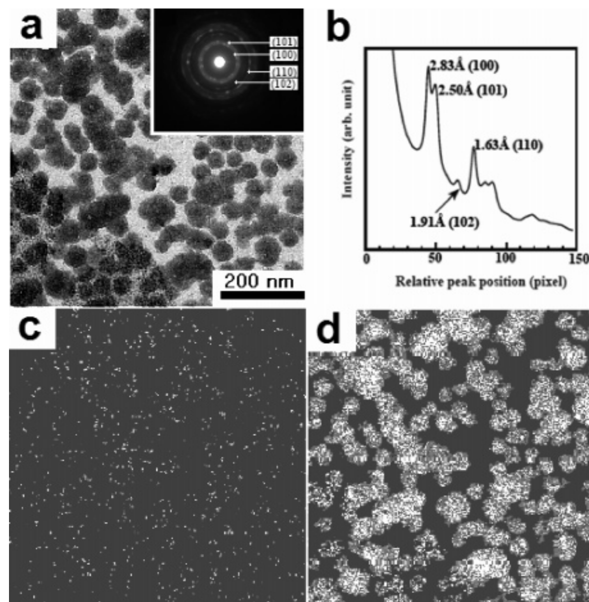

Figure 5. (a) A zero-loss image in EFTEM and the corresponding SAED pattern (inset) for the magnified ZnO particles prepared at 50 °C for 5 min in an aqueous solution of 0.05 M $Zn(NO_3)_2$ and 0.05 M DMAB, where Pd catalysts were prepared on the UV irradiated area by exposure to $Pd(acac)_2$ vapor for 5 min, (b) the intensity profile of the electron diffraction pattern, and (c) and (d) were the Pd and Zn elemental maps for the (a), respectively.

peaks for Pd element are 341.1 and 335.5 eV and BE of the O 1s peak in the carbonyl group of PMMA is 532.9 eV.[19] However, in spectrum (b) two Pd 3d peaks disappear and new peaks for Zn 2p in ZnO are found at 1045.5 eV for Zn $2p_{1/2}$ and 1022.3 eV for Zn $2p_{3/2}$ with a separation of 23.2 eV between the two peaks, which is in good agreement with the typical ZnO film.[20] Zn $2p_{3/2}$ is well-known as the characteristic peak for the Zn^{2+} in ZnO. The BE of the O 1s peak in the carbonyl group is replaced with the O 1s peak in ZnO at 530.2 eV.

To verify the ZnO deposition by EFTEM, SAED, and elemental mapping techniques, ZnO was synthesized on the Pd-patterned PMMA thin film at 50 °C for 5 min in the aqueous solution of 0.05 M $Zn(NO_3)_2$ and 0.05 M DMAB, where Pd patterned PMMA thin film was preliminarily prepared on the 600 mesh TEM copper grid, following the similar procedure explained above in Figure 2. A zero-loss image in EFTEM is shown in Figure 5a for the magnified ZnO nanoparticles in the UV irradiated area, which is the same image of the conventional TEM observation. Sphere-like ZnO nanoparticles with about 50 nm particle size contacted one another. The corresponding SAED ring pattern is also shown in the inset of Figure 5a and the intensity distribution curve shown in Figure 5b was calculated from the ring pattern. The peaks at 2.83, 2.50, 1.91, and 1.63 Å are assigned to (100), (101), (102), and (110) of ZnO wurtzite structure consisting of hexagonal lattice, respectively.[21] The elemental maps of Pd and Zn (Figure 5c and 5d, respectively) were obtained by EFTEM in which those maps were created by the "three-window method" using the two background

(19) Kim, K. J.; Lee, N. E.; Kim, M. C.; Boo, J. H. *Thin Solid Films* **2001**, *398*−*399*, 657−662.
(20) Islam, N.; Ghosh, T. B.; Chopra, K. L.; Acharya, H. N. *Thin Solid Films* **1996**, *280*, 20−25.
(21) *PCPDFWIN ver. 2.4*; International Centre for Diffraction Data: 2003.

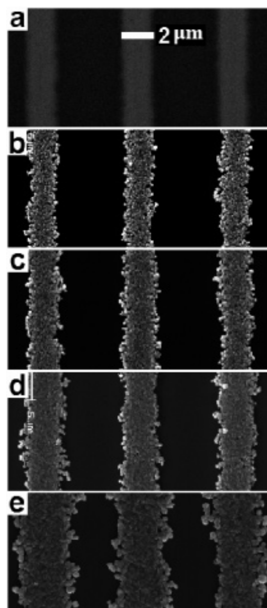

Figure 6. SEM images showing (a) Pd line (bright area) pattern whose exposure time to Pd(acac)$_2$ vapor was 5 min and (b)−(e) ZnO line patterns deposited on each Pd line pattern with different exposure times to Pd(acac)$_2$ vapor: (b) 3 min, (c) 5 min, (d) 10 min, and (e) 30 min. All ZnO patterns were synthesized at 50 °C for 20 min in an aqueous solution of 0.05 M Zn(NO$_3$)$_2$ and 0.05 M DMAB.

images at 295 ± 10 and 320 ± 10 eV and a core loss image at 415 ± 10 eV for the Pd map, and the two background images at 950 ± 20 and 980 ± 20 eV and a core loss image at 1150 ± 20 eV for the Zn map.[22] The maps of Pd and Zn were accurately overlapped to the zero-loss image and it confirmed that the ZnO particles were site-selectively deposited on Pd catalysts. The oxygen map also agreed with the Zn map, but it is not displayed here.

Figure 6 shows the effect of exposure time to Pd(acac)$_2$ vapor on the accuracy of ZnO line pattern. Figure 6a is the Pd line (bright area) pattern with ca. 2.0 μm width prepared by exposure to Pd(acac)$_2$ vapor for 5 min at 180 °C N$_2$ atmosphere, and we found that the Pd line width was not affected by the exposure time. ZnO line patterns in Figure 6b−e were fabricated on each Pd line pattern with the exposure time of (b) 3 min, (c) 5 min, (d) 10 min, and (e) 30 min, respectively. All ZnO patterns were synthesized at 50 °C for 20 min in an aqueous solution of 0.05 M Zn(NO$_3$)$_2$ and 0.05 M DMAB. Most ZnO crystals were deposited with an excellent site selectivity on the Pd patterns, and it implies that the Pd catalysts within the UV irradiated area have good catalytic activity. The line width of each ZnO pattern for Figure 6b−e was 1.8, 2.1, 2.3, and 2.9 μm, respectively. The line width increased with the increasing exposure time, and the optimum exposure time was 5 min, producing a dense ZnO film with accurate boundary. However, when the exposure time was 3 min, ZnO deposition density was poor, while the excessive width of ZnO line was formed at over 10 min of exposure time. It meant that many Pd nanoparticles of 3 min exposure were covered by PMMA film because of their small particle size; however, some Pd nanoparticles of over 10 min exposure were disclosed out of the boundary area.

(22) Reimer, L. *Energy-Filtering Transmission Electron Microscopy*; Springer: Münster, 1995; pp 347−400.

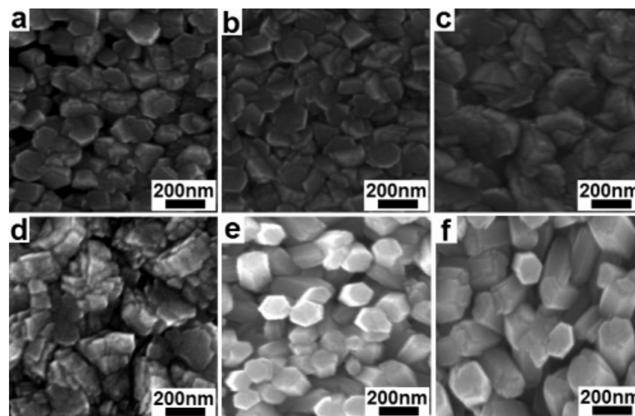

Figure 7. SEM images showing various morphologies of ZnO crystals. (a)−(d) were deposited at 50 °C for 20 min on the Pd catalysts with different exposure times to Pd(acac)$_2$ vapor for (a) 3, (b) 5, (c) 10, and (d) 30 min; (e, f) were deposited at 80 °C for 5 min on the Pd catalysts with different exposure times to Pd(acac)$_2$ vapor for (e) 5 and (f) 30 min.

Figure 7a−d shows the various morphologies of ZnO nanostructures deposited on the Pd catalysts prepared by exposure to Pd(acac)$_2$ vapor for (a) 3 min, (b) 5 min, (c) 10 min, and (d) 30 min, respectively. They were synthesized at 50 °C for 20 min in an aqueous solution of 0.05 M Zn(NO$_3$)$_2$ and 0.05 M DMAB. Figure 7e,f shows deposition on the Pd catalysts with (e) 5 min and (f) 30 min exposure time, where they were synthesized at 80 °C for 5 min in the same solution. As the exposure time increased, that is, as the average Pd particle size increased (Figure 2), short faceted hexagonal rods of ZnO became fatter and the roughness of the crystal surface became more complex at 50 °C. The crystals impinged and overlapped to the neighboring crystals, producing dense and ca. 200 nm thick films. However, long and smooth hexagonal rods grow at high temperature of 80 °C and they became a little fatter with the increasing Pd particle size. These results show that the crystalline morphology is drastically affected by the particle size of Pd catalysts and the deposition temperature. The former caused the fatter crystals, while the latter suppressed the lateral growth, giving the longer hexagonal nanorods.

We also studied the effect of deposition time on the change of crystal morphology by SEM observation, which was not shown here. In the early stage of crystal growth at 50 °C, the morphology of the ZnO crystals mostly consisted of rounded rectangular particles, and after 10 min, most of them were changed to short faceted hexagonal rods. And then, these hexagonal rods became fatter after 20 min. At 80 °C, hexagonal structures were generated under 1 min of very short reaction time and formed much thinner and longer hexagonal structures with increasing deposition time.

To understand the effects of various factors on the growth direction of ZnO crystals, the aspect ratio (length/diameter) of the crystals was estimated using image analyzer (Figure 8). In this stage, we observed them in the UV masked area because they could grow without the hindrance of one another but there was no difference to those deposited on the UV irradiated area except the deposition density. The aspect ratio increased with increasing deposition temperature,

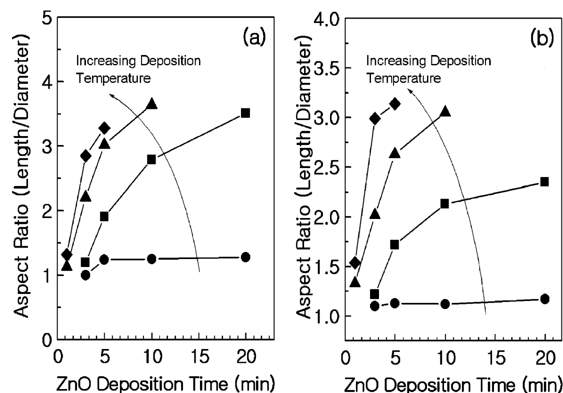

Figure 8. Effects of exposure time to Pd(acac)$_2$ vapor and deposition temperature on the aspect ratio (length/diameter) of ZnO crystals. Pd(acac)$_2$ exposure time: (a) 5 min and (b) 30 min; ZnO deposition temperature: (●) 50 °C, (■) 60 °C, (▲) 70 °C, and (◆) 80 °C.

regardless of exposure time to Pd(acac)$_2$ vapor. In the case of deposition at 50 °C, it was almost constant in all the deposition times, and it meant that the longitudinal growth rate and the lateral growth rate were almost the same. However, it was rapidly increased with increasing deposition temperature, which was due to the lateral growth being suppressed at high temperature. On the other hand, the aspect ratio decreased with increasing exposure time to Pd(acac)$_2$ from 5 min (Figure 8a) to 30 min (Figure 8b), and it meant that the particle size of the Pd catalyst promoted the lateral growth through the unification of ZnO crystals on large Pd particles.

Conclusions

Fine ZnO patterns were site-selectively grown on the Pd catalysts through the electroless deposition process under mild conditions, where photopatternable Pd catalysts were designed to be positioned on the surface of UV irradiated PMMA film via the reduction of vaporized Pd(acac)$_2$. The pattern accuracy and the crystalline morphology were drastically affected by Pd particle size and deposition temperature. As the Pd particle size increased, the line accuracy became poor and the morphology became fatter and rougher. The morphology of ZnO crystals deposited at 80 °C exhibited the hexagonal nanorods with high aspect ratio, while that of 50 °C was short faceted hexagonal nanorods. These suggested that the larger Pd catalysts caused the fatter ZnO crystals and the higher deposition temperature suppressed the lateral growth, giving longer hexagonal nanorods. The optimum ZnO pattern was obtained from the following conditions: ca. 20 nm PMMA film thickness, 20 J/cm^2 of UV dose, and 5 min of the exposure time to Pd(acac)$_2$. We will apply this technique to electron beam or block copolymer lithography in order to get higher resolution patterns.

Acknowledgment. J. Y. Lee thanks the Japan Society for the Promotion of Science (JSPS) for the postdoctoral fellowship.

CM0506555